A NEW ELECTRIC VEHICLE BATTERY CHARGING USING INDUCTIVE POWER TRANSFER TOPOLOGY

[1]P.Abdul Nabi,[2]Dr.K.Chithambaraiah Setty,[3]P.Pedda Reddy
[1]M.Tech Student,[2]Professor,[3]Associate Professor
Department Of EEE
St. Johns College of Engineering & Technology,Yerrakota

Abstract—Recently developed high-frequency power converter topologies for restricted power transfer range inductive power transfer (IPT) systems either use zero voltage switching (ZVS) or zero current switching (ZCS) based power electronic converters. It is still difficult to achieve ZVS or ZCS for all power switches at once in IPT systems. The enhanced zero-voltage zero-current trying to switch (ZVZCS) IPT architecture and its switching pattern are presented in this paper. In addition to using an auxiliary network to produce ZCS, ZVS is obtained by optimising the traditional series compensation. MATLAB/Simulink simulations for resistive and battery loads are used to validate the suggested approach. Last but not least, the outcomes achieved using a simulink rated for 1.1 kW, 85 kHz, demonstrate the practical practicality of the suggested topology. ZVZCS is able to transmit dynamic power between 20 W and 1.1 kW with an efficiency of 91.26 percent.

Index Terms— Electric vehicles (EVs), battery chargers, dc-dc power converters, wireless power transfer, inductive charging.

I.INTRODUCTION

The depletion of petroleum supplies and dangerous changes in the environment are two challenges confronting the increasingly global economy. Additionally, it has sparked the development of environmentally friendly technology that have improved significant carbon emitters like transportation [1], [2]. In order to lessen the environmental consequences of carbon-based fuels, electric vehicles (EVs) are already widely utilised [2, 3]. Additionally, the market for EVs provides a new chance for people to extend the lifespan of transportation at a reduced cost [1], [3]. In the past, EV commercial performance has been hindered by limits in battery technology (BT) and power shaping technologies. However, over the course of the last several decades, BT has developed to have a high energy density, a low weight, and a high efficiency [4]. Additionally, when utilised with an appropriate power shaping circuit, an efficient energy storage device enhances overall performance. Researchers and businesses have experimented with a dc-dc power conditioning system with lower power losses, durability, consistent energy transmission, and enhanced charging-discharging cycles [1]–[4]. With concerns for human safety, efficient, quick chargers are being used for short driving distances. As safer battery charging (BC) solutions for EV stationary and dynamic mode, inductive power transfer (IPT)-based typologies are employed in the current situation. In order to increase the converter's overall efficiency, compensation networks are offered to reduce the circuit impedance. However, the complexity of the setup is correlated with the number of active and passive circuit parts [5].

The ideal solution enhances the driving range, maintenance cycle, carbon footprint reduction, and end-user economics. Therefore, the choice of converter is crucial to the market's EV flow. As a result, it skillfully assists reduction in environmental difficulties brought on by transportation challenges [6]. Due to its simple construction and operational stability for varied coil distances, the traditional series-series capacitor compensation based IPT topology is one of the most popular network arrangements used by businesses [7]. The efficiency, power transmission ability, strong resonant peaks, and control precision for variation loading are all compromised by this network's cheap cost.

An method for phase control is provided in [7] to increase bandwidth efficiency, however the cost comes from a complex control technique for a different frequency. By setting the control border in the ideal frequency range, [8] addresses problems brought on by fluctuating frequency. The control strategies discussed in [7] and [8] only help significantly to maintain zero voltage switching (ZVS) for IPT system and give improved efficiency. A novel coil support network utilising an intermediate L-C series compensated structure at both the transmitter and receiver ends has achieved the topological progress in [9]. By positioning both coils on the main side in [10], this layout reduces weight at the vehicle side. However, the beauty of simplicity in calculation and control operation is diminished by the solution described in [9] and [10], which supports magnetic flux in a misaligned situation. In [11], the problems associated with using

an isolated tank network to support IPT are resolved by combining an H-bridge high-frequency transformer with an L-C tank network. However, it decreases peak efficiency while expanding the system's size, weight, and volume. The restoration of the passive component's network is therefore proposed in [12]–[17] as a remedy to address problems caused by the inclusion of a second magnetically separated resonant tank. In order to increase the system's performance over an extended period of time, symmetrical filter networks with loosely connected transformer coils are cascaded in [12] and [13]. The use of magnetically separated inductors in these topologies, however, increases weight, volume, the complexity of the tuning procedure, and reduces efficiency. When adopting the LCC-C network design, asymmetrical compensation is used to overcome these problems in [14] and [15]. In [16] and [17], the comparison of the analyses of the assertions in [12] to [15] reveals that, for the identical coil design, the LCC-LCC network is adequate for stationary IPT and the LCC-C network for dynamic IPT.

However, it experiences distortions when there are changes in clearance and vehicle side topology. Therefore, using series C-C compensation, Zhang et al. [16] and Li et al. [17] set out to develop an alternative approach. In [18]–[20], a method to increase the performance and efficiency of the strongly coupled transformer-based dc–dc converter by stabilising soft switching is provided. The auxiliary network is used in [21] and [22] to improve the performance of the resonant IPT topology based on [18]-[20]. Due to the installation of more magnetics, the constant losses have risen while still achieving steady operation and increasing efficiency. Similar to this, [23] presents a solution for a series C-C compensated topology based on resonant IPT. According to this perspective, IPT with an extra circuit may help a network powered by a voltage source inverter (VSI) fed converter deal with several problems. This article proposes a topology that combines zero current switching (ZCS) with ZVS using traditional series L-C compensation and modest auxiliary components. Even when the input is exposed to a broad range of voltage changes, the suggested design provides a consistent output voltage. The cost of the converter is effectively decreased since the output current may be readily regulated from the input side voltage, negating the need for a high-power CPU to manage operation. A lab prototype has been created and tested for battery and resistive load throughout the whole BC range. Fig. 1 depicts the overall architecture that has been presented, in which two stages of the converter have been independently regulated using modified pulsewidth modulation (MPWM). To accomplish zero-voltage zero-current switching (ZVZCS) and supply power up to 1.1 kW, the pulses are produced at an 85 kHz switching frequency in MPWM mode. Performance data are shown.

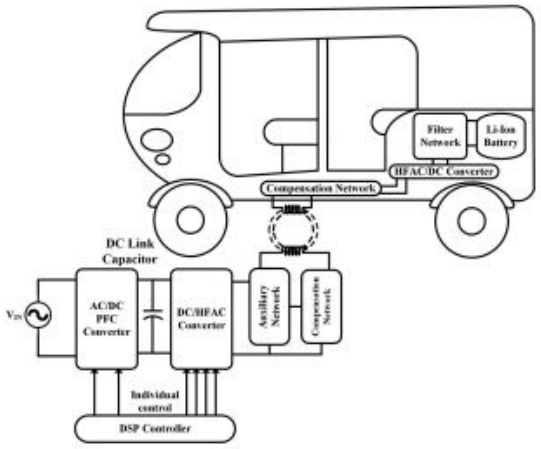

Fig. 1. General configuration of wireless battery charger topology

II.ELECTRIC VEHICLE

An electric vehicle, often known as an EV, propels itself using one or more electric motors or traction motors. An electric vehicle may be self-contained with a battery, solar panels, or an electric generator to convert gasoline to energy, or it may be fueled via a collector system by electricity from off-vehicle sources. [1] Road and rail cars, surface and underwater watercraft, electric aeroplanes, and electric spacecraft are just a few examples of EVs.

EVs first appeared in the middle of the 19th century, when electricity was one of the most popular forms of motor vehicle power. They offered a degree of comfort and convenience of use that gasoline automobiles of the day were unable to match. For over a century, modern internal combustion engines have dominated the propulsion of motor vehicles, but electric power has remained prevalent in other vehicle types, including railways and smaller vehicles of various kinds.

Due to advancements in technology and a greater emphasis on renewable energy sources, EVs had a renaissance in the twenty-first century. A small group of do-it-yourself (DIY) engineers started exchanging technical information for doing electric car conversions as there was a significant increase in demand for electric automobiles. Governmental incentives to boost adoptions have been implemented, especially in the US and the EU.

Edison and a 1914 Detroit Electricmodel 47 (courtesy of the National Museum of American History)

An EV and an antique car on display at a 1912 auto show

III.POWER FACTOR

Alternating current is virtually always used to create, transfer, and distribute electrical energy. As a result, the power factor issue is instantly raised. Since the majority of loads (such as arc lights and induction motors) are inductive in nature, their lagging power factors are often low. Because it increases current and results in increased active power losses in all components of the power system, from the generator at the power plant down to the utilisation devices, the low power factor is very unfavourable. A supply system should have a power factor that is as near to unity as feasible to provide the technical and financial circumstances that are most advantageous. We'll talk about many ways to boost power factor in this chapter.

In an a.c. circuit, power factor is the sine of the angle between voltage and current. The phase mismatch between voltage and current in an a.c. circuit is often present. Circuit power factor is referred to by the symbol cos. The power factor is referred to as trailing if the circuit is inductive because the current trails the voltage. Although power factor is supposed to be leading, current in a capacitive circuit leads the voltage. Think about an inductive circuit that receives a lagging current I from a supply voltage V, where the angle of lag is. In Fig. 6.1, the circuit's phasor diagram is shown.

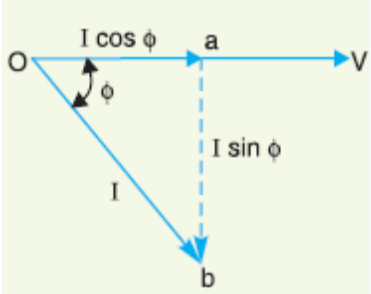

Fig. 6.1

It is possible to divide the circuit current I into two perpendicular halves, namely
(a) I cos in phase with V.
(b) I'm 90 degrees out of phase with V .

PULSE WIDTH MODULATION

Pulse Width Modulation By switching the solar system controller's power devices, (PWM) is the most efficient way to achieve constant voltage battery charging. When using PWM control, the solar array's current tapers in accordance with the battery's state and recharge requirements. Think about the following waveform: The voltage is switched between 0 volts and 12 volts. It should be very evident that a "appropriate device" attached to its output would perceive the average voltage and believe it is being fed 6v, which is precisely half of 12v, as the voltage is at 12v for exactly as long as it is at 0v. Consequently, we may change the "average" voltage by adjusting the width of the positive pulse.

Also, if the switches maintain the voltage at 12 for

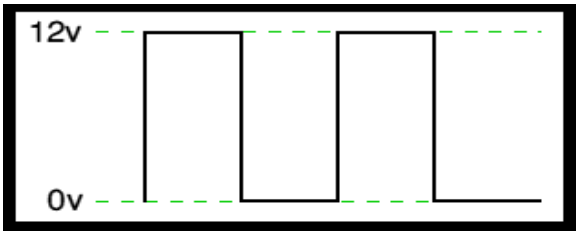

three As seen below, the average voltage will be around 3/4 of 12 volts, or 9 volts.

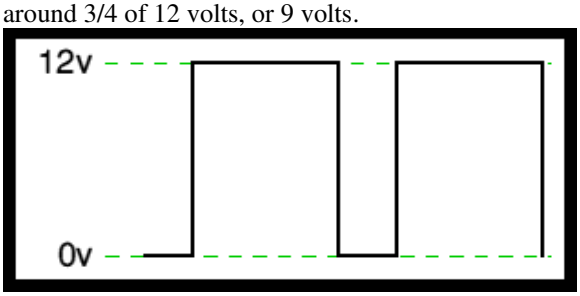

Moreover, if the output pulse of 12 volts lasts just 25% of the whole duration, the average is

IV.PROJECT DESCRIPTION AND CONTROL DESIGN

OPERATING PRINCIPLE OF THE PROPOSED CONVERTER

A H-bridge is formed of active switches S1–S4 on the main side and diodes D5–D8 on the secondary side (conventional). Additionally, to retain the soft-switching property of the circuit with BC, Ca1 and Ca2 function as potential dividers at the input with ancillaryLA and TA. L1 and L2 are connected to C1 and C2 on the circuit's main and secondary sides, respectively. Using MPWM, the converter's operation is managed in [22]. To comprehend the suggested converter's functioning concept, the following presumptions are taken into account. 1) The transformer, dc source, switches, diodes, capacitors, internal switch diode, and capacitance are all excellent active and passive devices. 2) The interwinding capacitance of the transformer and the electrical series resistance of the inductor are disregarded. 3) The converter's input and output terminals may maintain a constant voltage thanks to the voltage divider capacitors (Ca = Ca1 = Ca2) and CF. 4) The consequences of TA's magnetising inductance are disregarded.

A. Operation of Proposed Converter

The suggested topology's steady state working principle is separated into eight modes (modes I–VIII), as illustrated in Fig. 2, and the operational waveforms are shown in Fig. 3. Fig. 2(a), Mode I (t0 t t1): Lagging current (IL1 + ILA) is flowing from D1 and S2 prior to time instant t0; as a result, the switch S1 is switched ON with ZVS at this instant. Additionally, a prospective gap between AC and CB is established, and current ILA begin to rise from ILA(t0).

$$i_{L_A} = \begin{cases} \text{If} \rightarrow R_{ON(S_1-S_4)} \neq 0 \\ \dfrac{|V_{C_{a1}} - V_{C_{a2}}|}{2L_A} T_{\text{ON}} - i_{L_A(t_0)} \\ |V_{C_{a1}} - V_{C_{a2}}| = 0 \;||\; i_{L_A} = 0 \end{cases} \begin{cases} \\ \\ \text{If} \rightarrow R_{ON(S_1-S_4)} = 0 \end{cases}.$$

Fig. 2(b) and (c), Mode II (t1 t t2): Switch S1 is conducting before time zero (t0), and switch current difference (iS1 iS2) is flowing from the time source TA (ITA1 + ITA2 = ILA). iCS1 + iCS4 = iTA2 + iL1 (2) 2iCS1 = iL1 + iLA 2 when minimal energy conservation is used and KCL is applied at sites A and B. (3) S1 is switched OFF at the beginning of this mode while S3, S4, and S2 are already off and S2 is still conducting. Now that the dominating inductance L1 is disconnected from the dc power supply, the switch peracetic capacitor CS1 is being charged by IL1 + ILA 2. When t11 occurs, VCS1 reaches VDC. IL1 discovers a route after t11 by causing the change in ILA . This change is rejected by the inductor LA, and a current flows from S2 to S4 to discharge CS4. D4 goes on when the CS4 voltage drops to zero, which causes IS2 to decrease to zero or ZCS for switch S2 t (VCS1=VDC) = 1 2CS3VDC iL1(t1) + iLA(t1) 2 iL1(t) + iLA (t) 2 . (4) Fig. 2(d) and (e) show Mode III (t2 t t3). While all other switches are already off, this mode begins when S2 ZCS is turned off. The current ILA decreases toward zero after reaching its positive peak during this phase, and the peracetic capacitor CS2 begins charging until t21 up to VDC. After t21, the current IL1 + ILA 2 finds its course by discharging capacitors CS3, CS4, and turning ON the diodes D2, D4. t1 > 2CS1 VDC iL1(t0) + iLA(t0) 2 are then turned ON. (5) The formula that follows gives the voltage stress across the switch: (6) vS1 = VDC + vC1; vS4 = vC1. (7) 4) Mode IV (t3 t t4), Fig. 2(f): S4 is switched ON with ZVS as D4 is on, and the voltage across S4 is almost zero. After reaching its negative peak, the auxiliary inductor current ILA is growing linearly in the positive direction. 5) S3 is switched ON with ZVS in Mode V (t4 t t t5), seen in Fig. 2(g). Voltage across S3, S4 are zero when IAB begins to follow the sinusoidal wave pattern, indicating that its course has been finished. Mode VI (t5 t t t6), seen in Figs. 2(h) and I begins by shutting off S3, which causes CS3 to begin charging up to VDC att51. When ZCS is turned off, IS4 must decrease due to the auxiliary inductor current ILA's declining trend after reaching its peak.

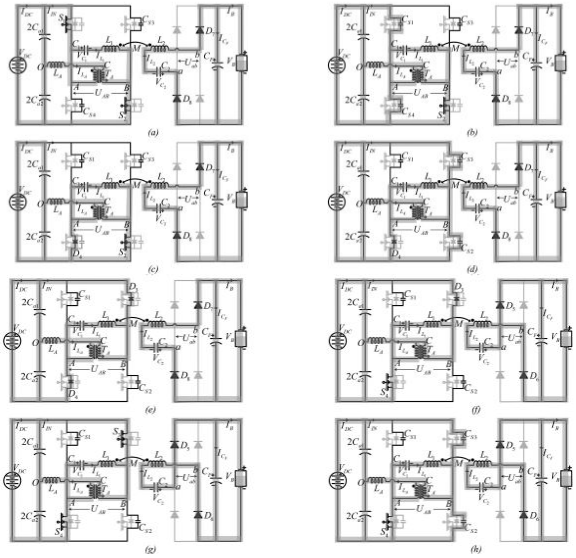

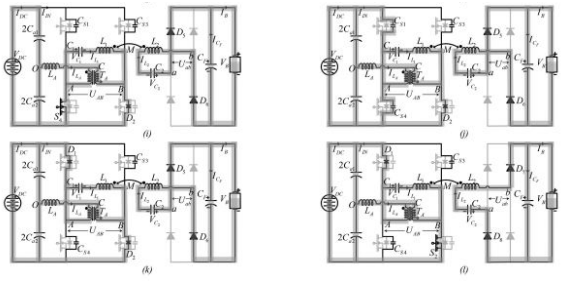

Fig. 2. Operating modes of proposed battery charger topology. (a) Mode I (t0 ≤ t < t1). (b) Mode II (part-1) (t1 ≤ t < t11). (c) Mode II (part-2) (t11 ≤ t < t2). (d) Mode III (part-1) (t2 ≤ t < t21). (e) Mode III (part-2) (t21 ≤ t < t3). (f) Mode IV (t3 ≤ t < t4). (g) Mode V (t4 ≤ t < t5). (h) Mode VI (part-1) (t5 ≤ t < t51). (i) Mode VI (part-2) (t51 ≤ t < t6). (j) Mode VII (part-1) (t6 ≤ t < t61). (k) Mode VII (part-2) (t61 ≤ t < t7). (l) Mode VIII (t7 ≤ t < t8).

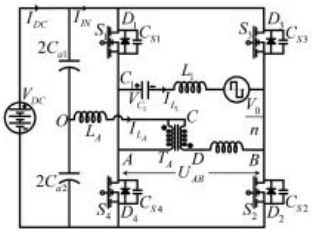

Fig. 4. Simplified network with battery load refereed at transmitter coil side.

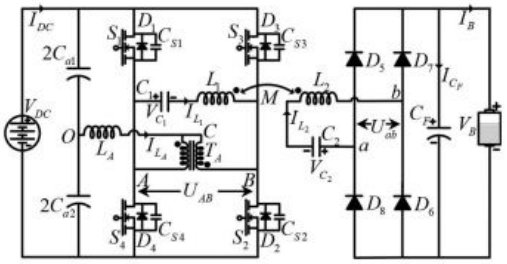

Fig. 5. Proposed network configuration of EV battery charger.

7) Mode VII (t6 ≤ t < t7), Fig. 2(j) and (k): S4 is shut off at ZCS in this mode, and VCS4 climbs to VDC att 61. After minute 61, ILA begins to incriminate in a favourable manner. Power is sent back to the source once the diodes D1 and D2 are switched on.

8) Mode VIII (t7 ≤ t < t8), Fig. 2(l): Transfer S2 is activated with ZVS in this mode of operation, causing current to switch from D2 to S2. Battery voltage and current are kept constant in modes I through VIII.

V.RESULTS AND DISCUSSION

By using modelling, simulation, and hardware testing, the suggested converter topology's operating principle is confirmed. To understand the behaviour of the converter, simulation and hardware circuit settings are adjusted to an operational point. A. Results of the Simulation Principal component analysis was used in MATLAB/Simulink to simulate a suggested topology, as illustrated in Fig. 10. In Fig. 4 and Table I, ZVS turn-ON for S1–S4. The optimum DC source is connected in series with an inductor and resistor (n) (nH). To replicate the H-bridge portion of the dc-dc converter, MOSFET switches from the SimPowerSystem Library with 0 resistance and 870 pF capacitance as snubber were utilised. From mutual inductance, the linear transformer, transmitter, and reception coils contract the auxiliary transformer. As the voltage across the switch drops to zero, the gate pulse is sent to that specific switch to turn it ON. This is shown in Fig. 10 for the ZVS turn-ON of switches S1 through S4. The ZCS turn-ON for switches S2 and S4 is shown in Fig. 11(a) and (b). Before the gate pulse is finished, the switch's current drops to zero. The suggested wireless converter is hence said to maintain ZCZVS. By evaluating the performance of VC1, as seen in Fig. 12, the compensating capacitor voltage peak value is chosen. The input side characteristic of the main network is shown in Fig. 13. These findings demonstrate that the converter's performance is unaffected by the tiny value of the input dc-link capacitors. Fig. 14(a)- displays the converter's performance for BC (d). As can be seen from Fig. 14(a) and (b), there is very little disturbance. In contrast, the conventional charger causes disturbances in BC voltage and current, which shortens battery life and reduces charger efficiency. In contrast, the battery voltage and current in Fig. 14(c) and (d) are shown without the use of an auxiliary circuit. With the specifications, the circuit's performance offers 93.5 percent efficiency.

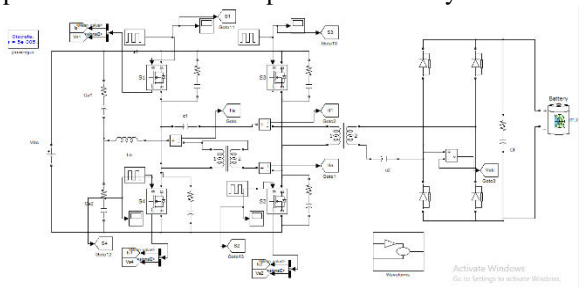

Fig: Proposed Simulation Diagram

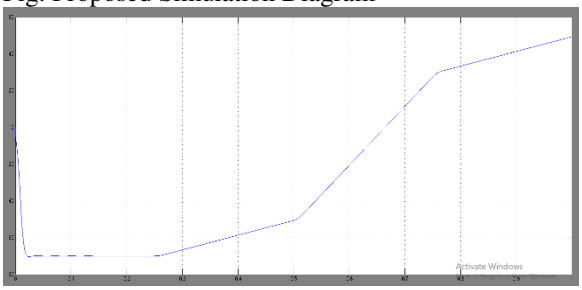

Fig: Il1

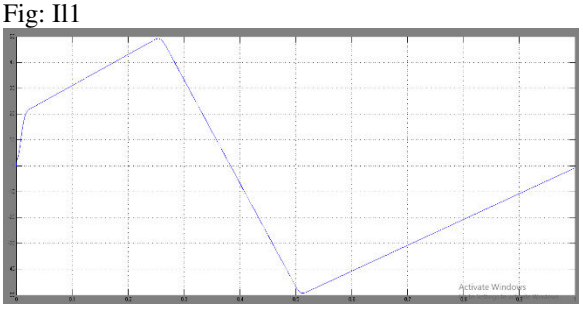

Fig: Ila

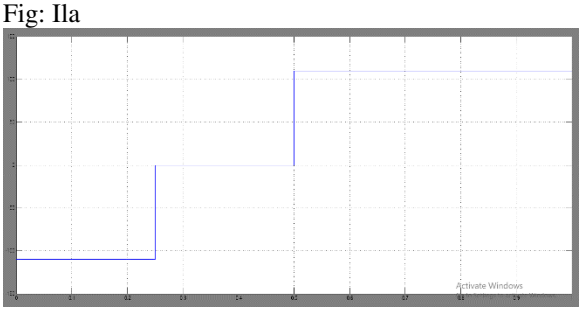

Fig: Vab

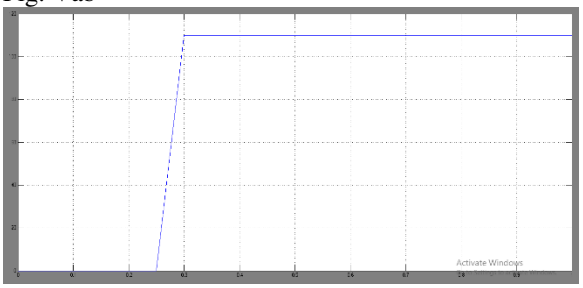

Fig: Vs1

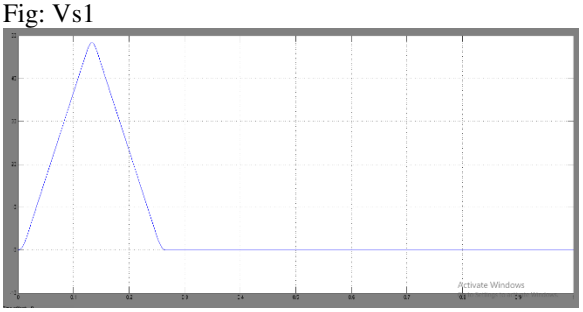

Fig: Is1

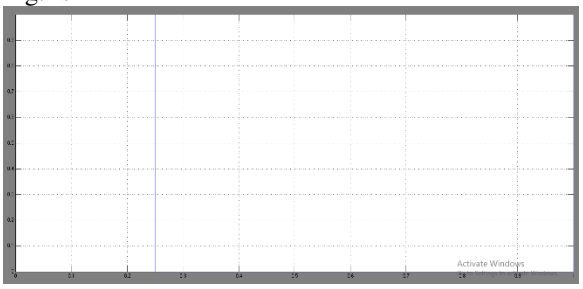

Fig: S1

CONCLUSION

This article proposes a wireless electrical vehicle battery charger architecture based on voltage fed series compensation and its tuning approach. The full-bridge dc-dc converter has improved performance with a broad range of input variation thanks to improvements that were appropriately suggested. Eliminating the need for a high-power CPU lowers the cost overall. To achieve ZVZCS with less control complexity, theoretical analysis and modelling have been given. The simulation results confirmed the suggested topology's ZVZCS condition over the whole load range. Utilizing low values for the dc link and filter capacitance, respectively, the proposed approach reduced input/output voltage and current ripple. For battery and resistive loads, a satisfactory efficiency of 91.26 percent has been attained.

REFERENCES

[1] M. Granovskii, I. Dincer, and M. A. Rosen, “Economic and environmental comparison of conventional, hybrid, electric and hydrogen fuel cell vehicles,” J. Power Sources, vol. 159, no. 2, pp. 1186–1193, 2006.

[2] S. B. Peterson, J. Whitacre, and J. Apt, “The economics of using plug-in hybrid electric vehicle battery packs for grid storage,” J. Power Sources, vol. 195, no. 8, pp. 2377–2384, 2010.

[3] Y. Zhou, M. Wang, H. Hao, L. Johnson, and H. Wang, “Plug-in electric vehicle market penetration and incentives: A global review,” Mitigation Adaptation Strategies Global Change, vol. 20, no. 5, pp. 777–795, 2015.

[4] B. Nykvist and M. Nilsson, “Rapidly falling costs of battery packs for electric vehicles,” Nature Climate Change, vol. 5, no. 4, pp. 329–332, 2015.

[5] W. Zhang and C. C. Mi, “Compensation topologies of high-power wireless power transfer systems,” IEEE Trans. Veh. Technol., vol. 65, no. 6, pp. 4768–4778, Jun. 2016.

[6] K. Mude and K. Aditya, “Comprehensive review and analysis of two-element resonant compensation topologies for wireless inductive power transfer systems,” Chin. J. Elect. Eng., vol. 5, no. 2, pp. 14–31, 2019.

[7] Y. Jiang, L. Wang, Y. Wang, J. Liu, X. Li, and G. Ning, “Analysis, design, and implementation of accurate ZVS angle control for EV battery charging in wireless high-power transfer,” IEEE Trans. Ind. Electron., vol. 66, no. 5, pp. 4075–4085, May 2019.

[8] Y. Jiang, L. Wang, Y. Wang, J. Liu, M. Wu, and G. Ning, “Analysis, design, and implementation of WPT system for EV’s battery charging based on optimal operation frequency range,” IEEE Trans. Power Electron., vol. 34, no. 7, pp. 6890–6905, Jul. 2019.

[9] D. H. Tran, V. B. Vu, and W. Choi, “Design of a high-efficiency wireless power transfer system with intermediate coils for the on-board

chargers of electric vehicles," IEEE Trans. Power Electron., vol. 33, no. 1, pp. 175–187, Jan. 2018.

[10] S. Moon and G.-W. Moon, "Wireless power transfer system with an asymmetric four-coil resonator for electric vehicle battery chargers," IEEE Trans. Power Electron., vol. 31, no. 10, pp. 6844–6854, Oct. 2016.